Si/SiN Microring-Based Optical Router in Switch-and-Select Topology

Qixiang Cheng(1), Liang Yuan Dai(1), Meisam Bahadori(1), Nathan C. Abrams(1), Padraic E. Morrissey(2), Madeleine Glick(1), Peter O'Brien(2), Keren Bergman(1)

(1) Department of Electrical Engineering, Columbia University; New York, USA, qc2228@columbia.edu
(2) Tyndall National Institute, University College Cork, Cork Ireland

Abstract *We present the first strictly non-blocking optical switch in switch-and-select topology using microring resonators. The 4x4-port device incorporates thermally-actuated silicon microrings and Si/SiN two-layered central shuffle network, exhibiting on-chip loss and crosstalk ratio as low as 1.8dB and -50dB, respectively.*

Introduction

Modern datacenters increasingly rely on the optical interconnect for delivering critical communication connectivity among numerous servers. The photonic switch is considered a potential key element to meet the growing interconnection performance requirements in datacenter architectures[1]. Integrated photonic switch fabrics have been extensively explored in Indium Phosphide[2] and silicon[3-5] platforms. Benefiting from the CMOS industry's developed fabrication and manufacturing infrastructures, silicon photonic devices have quickly matured to see monolithic integration of tens of thousands of components[4]. Because of their small footprint and low power consumption, silicon microring resonators (MRRs) have been extensively studied as modulators, filters, and (de-)multiplexers. To date, MRR-based optical switches have been implemented using a crossbar architecture, which takes advantage of the add-drop feature of MRR cells.

In this work, we present the first monolithic optical switch fabric in switch-and-select (S&S) topology using MRRs. This device has 4x4 port count and incorporates 32 thermally-actuated silicon MRRs and a two-layered Si/SiN central shuffle network. On-state and off-state power transfer functions reveal that both switch crosstalk suppression and extinction ratio are up to >50 dB, due to the S&S topology. Optical connections are characterized, showing the switch on-chip loss as low as 1.8 dB with ~24 GHz optical bandwidth.

Topology

The S&S topology was first implemented in the MZI-based switch fabric[3]. The input and output switch arrays are built from individual 1xN switch units. Each switch unit is arranged in 1xN cascading structure with MZI cells, as illustrated by Fig. 1a. This can be considerably simplified by using MRR add-drop components assembled in

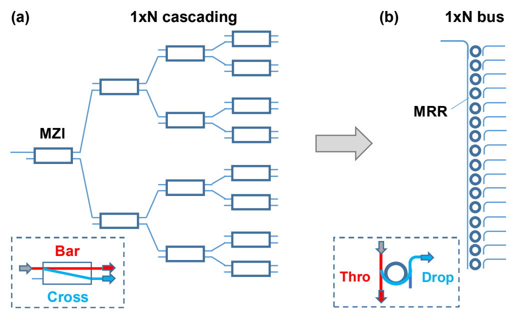

Fig. 1: (a) 1x16 MZI switch cascading structure, and (b) 1x16 MRR-based bus structure.

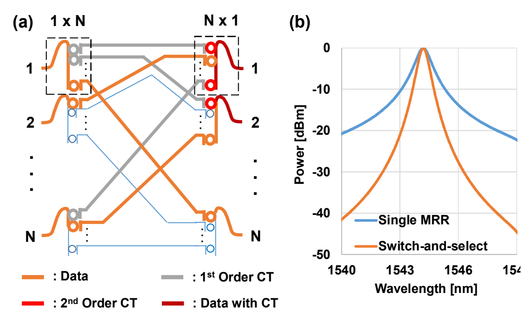

Fig. 2: (a) MRR-based switch-and-select topology, and (b) Drop spectrum of a single MRR element and the switch-and-select device.

a 1xN bus coupled structure, as shown in Fig. 1b.

Scaling the MRR-based S&S only requires adding microrings to the bus waveguides, which effectively reduces the scaling overhead in loss compared to that of the cascading scheme. The layout of a generic NxN-port S&S MRR-based switch is depicted in Fig. 2a[5]. This configuration has N input spatial 1×N and N output spatial N×1 units, maintaining the number of drop (i.e. resonating) microrings in any path at two. An NxN S&S switch requires in total $2N^2$ MRR elements.

The central passive shuffle connects the i^{th} ring (A) in the j^{th} 1×N input unit to the j^{th} ring (B) in the i^{th} N×1 output element. This brings a further advantage of self-routing as the optical connection of input *i* to output *j* occurs only when

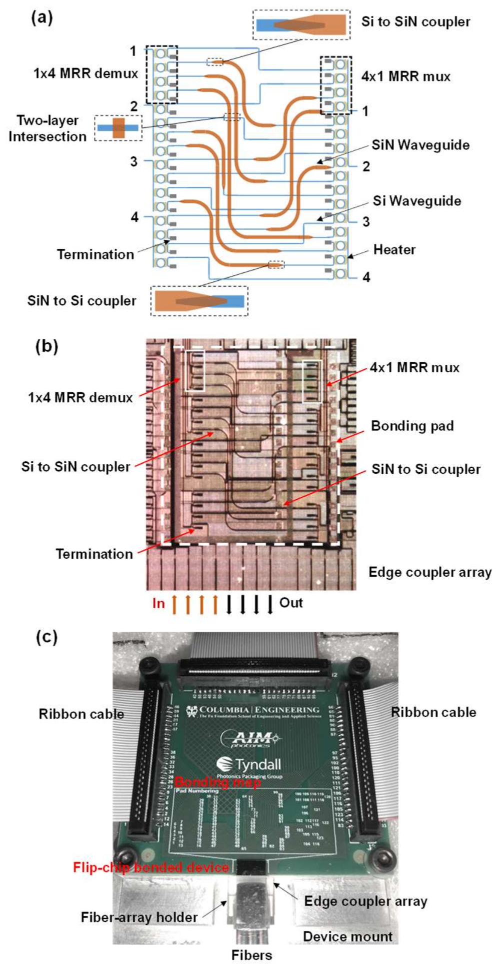

Fig. 3: (a) Schematic of the 4x4 Si/SiN MRR-based switch fabric. (b) Microscope photo of the fabricated device. (c) Packaged switch device by flip-chip bonding on the breakout PCB board.

both A and B rings are in the drop state (on resonance). The rest of the MRRs on the input and output units are adequately detuned from the drop state to ensure the maximum crosstalk suppression. This topology blocks the first-order crosstalk, which is reflected in the sharper spectral edge compared to that of the single MRR as presented in Fig. 2b.

Device design, fabrication and packaging

In this work, the add-drop MRR element is designed to operate close to its critical coupling to maximize the extinction of resonance and minimize the drop loss. Detailed design space exploration of silicon MRRs can be found in Bahadori et al.[6]. The tuning of the microrings is accomplished through an integrated micro-heater and the measured shift of resonance shows a thermal efficiency of 1 nm/mW[7].

A schematic of the 4×4 thermo-optic MRR-based S&S device is shown in Fig. 3a. Terminations are placed at the through port of ring resonators to eliminate optical reflections. The central shuffle network is implemented in a Si/SiN dual-layer structure with interlayer couplers, enabling a SiN waveguide to pass over a Si waveguide at intersections. Key parameters for such a dual-layer device include the width of SiN waveguide and the separation between the two layers, determining the mode interaction and thus the loss and interlayer crosstalk. An edge coupler array is used at a pitch of 127 um.

The device was taped out using standard PDK elements through the AIM Photonics MPW run. The 4x4 switch fabric (shown in Fig. 3b) has a compact footprint of 1.5×2.4 mm^2 with 32 control electrodes and 2 common grounds. The bare die was flip-chip bonded onto a PCB breakout board at Tyndall National Institute as shown by the photo in Fig. 3c. Limited by the size of the electrical trace/gap on the multi-layer PCB, only 28 out of the total 32 microrings were electrically fanned out, allowing a full control of 12 optical connections. A single-mode cleaved fiber array was attached by UV-cured glue to couple light into and out of the whole chip. Two pairs of looped-back edge couplers were introduced to facilitate the coupling process and determine the coupling loss, at ~5.3 dB/facet, as a reference.

Device characterization

Power transfer functions of the switch circuit are first assessed to verify the device physical layer performance. The experimental test-bed is schematically shown in Fig. 4. A tunable laser is used to launch a continuous-wave signal at the wavelength of 1542.3 nm at each input. The operating wavelength is selected to be close to the half FSR of MRRs to the resonance. The output is connected to an optical spectrum analyzer to record both the peak transfer power and the spectrum.

The switch fabric currently features a large path-dependent loss, which can be attributed to the high excess loss of interlayer couplers. Optical paths routed only in the silicon layer exhibit on-chip losses in the range of 1.8 to 3.0 dB. The losses increase to >11 dB for paths going through both Si and SiN layers. Test structures (presented in Fig. 5) show that a pair of Si-to-SiN and SiN-to-Si interlayer couplers

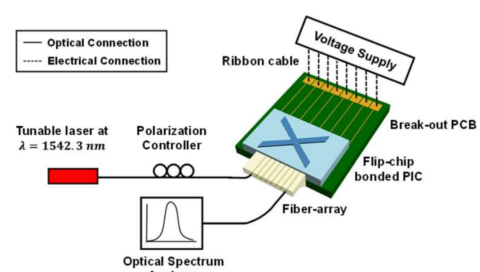

Fig. 4: Schematic of the device testbed.

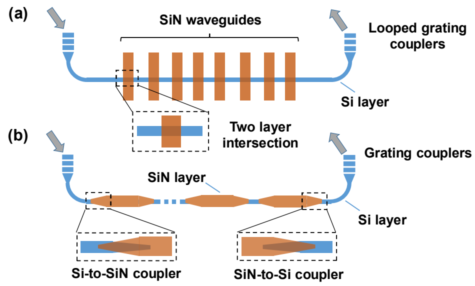

Fig. 5: Test structures of (a) Si/SiN two-layered intersections and (b) interlayer couplers.

encounters an insertion loss of ~4 dB. It is suspected that the SiN waveguide and bend structure bring about excess loss. This requires further investigation. Figure 6 shows detailed measurements on three representative paths, 4-4 in silicon layer, 2-2 in silicon layer under passing SiN waveguides and 2-3 shuffling through both layers. Referring back to Fig. 3a, optical path 4-4 incorporates three off-resonance MRRs and two on-resonance ones with no interaction with the SiN layer resulting in the optimal case. The 1.8 dB on-chip loss with -54.4 dB crosstalk ratio and 52.7 dB extinction ratio, shown in Fig. 6a and 6d, indicate the outstanding performance of the microring elements. The slight additional insertion loss for path 2-2 is due to the mode interaction with the SiN waveguide. The optical path 2-3 shown here represents the worst-case. It comprises an additional pair of interlayer couplers and 5 intersections giving rise to an extra ~19 dB loss due to the fabrication variation. The high insertion loss also factors into the degraded crosstalk (-31.6 dB) and extinction ratios (31.4 dB). This, however, can be significantly improved by optimizing the component design and fabrication uniformity. Bandwidth spectra of each path are subsequently measured using a broadband light source. Measured spectra of path 4-4, 2-2 and 2-3 are included in Fig. 6b, 6d and 6f respectively as insets, showing the passband of ~24 GHz.

Conclusions

The first microring-based Si/SiN optical router in switch-and-select topology is presented. The thermally-actuated 4x4-port device is fully packaged via flip-chip bonding. Power transfer function reveals the on-chip loss is down to 1.8 dB, with both crosstalk suppression and extinction ratio as high as >50 dB. This device shows great potential for high-performance switching applications in datacenters.

Acknowledgements

This material is based on research sponsored by Air Force Research Laboratory under agreement number FA8650-15-2-5220, ARPA-E ENLITENED project with contract number DE-AR00000843, and European Packaging Pilot Line 'PIXAPP' (H2020-731954).

References

[1] K. Bergman et al., Photonic network-on-chip design, Springer (2014).

[2] Q. Cheng et al., "The feasibility of building a 64×64 port count SOA-based optical switch," in Proc. Photonics in Switching (PS), Florence, pp. 199-201 (2015).

[3] L. Chen et al., "Compact, low-loss and low-power 8×8 broadband silicon optical switch," Opt. Express 20, 18977-18985 (2012).

[4] K. Tanizawa et al., "Ultra-compact 32 × 32 strictly-non-blocking Si-wire optical switch with fan-out LGA interposer," Opt. Express 23, 17599-17606 (2015).

[5] Q. Cheng et al., "Highly-scalable, low-crosstalk architecture for ring-based optical space switch fabrics," IEEE OI Conference, Santa Fe, NM, pp. 41-42 (2017).

[6] M. Bahadori et al., "Design Space Exploration of Microring Resonators in Silicon Photonic Interconnects: Impact of the Ring Curvature", IEEE JLT, 2018 [*in press*]

[7] M. Bahadori et al., "Thermal Rectification of Integrated Microheaters for Microring Resonators in Silicon Photonics Platform," IEEE JLT, 36, 3, 773-788 (2018).

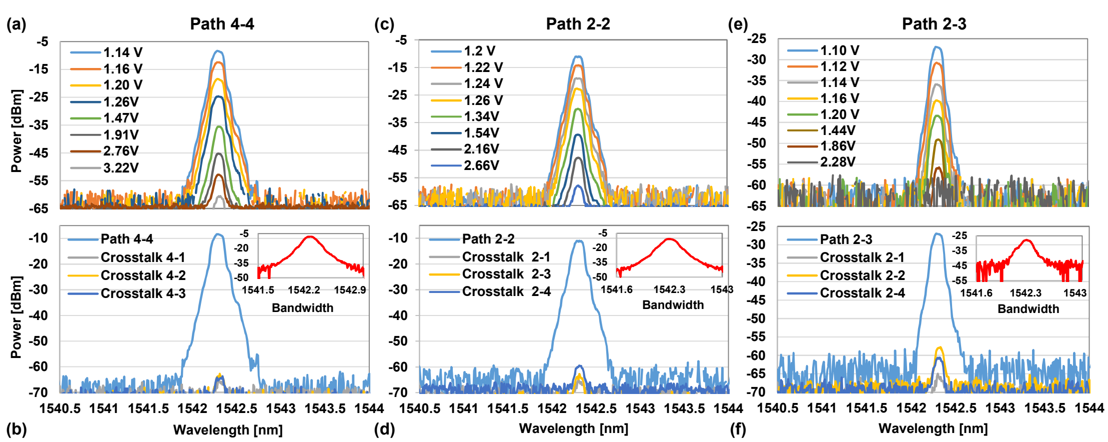

Fig. 6: Optical power vs. tuning voltage on the MRR at output stage for (a) path 4-4, (b) path 2-2 and (c) path 2-3. The difference between peak and minimum power reveals the path extinction ratio. Output power vs crosstalk leakage for (d) path 4-4, (e) path 2-2 and (f) path 2-3. Insets show bandwidth spectra for each path.